

# Magnon-Skyrmion Hybrid Quantum Systems: Tailoring Interactions via Magnons

Xue-Feng Pan,<sup>1</sup> Peng-Bo Li,<sup>1,\*</sup> Xin-Lei Hei,<sup>1</sup> Xichao Zhang,<sup>2</sup> Masahito Mochizuki,<sup>2</sup> Fu-Li Li,<sup>1</sup> and Franco Nori<sup>3,4,5</sup>

<sup>1</sup>Ministry of Education Key Laboratory for Nonequilibrium Synthesis and Modulation of Condensed Matter, Shaanxi Province Key Laboratory of Quantum Information and Quantum Optoelectronic Devices, School of Physics, Xi'an Jiaotong University, Xi'an 710049, China

<sup>2</sup>Department of Applied Physics, Waseda University, Okubo, Shinjuku-ku, Tokyo 169-8555, Japan

<sup>3</sup>Theoretical Quantum Physics Laboratory, Cluster for Pioneering Research, RIKEN, Wakoshi, Saitama 351-0198, Japan

<sup>4</sup>Center for Quantum Computing, RIKEN, Wakoshi, Saitama 351-0198, Japan

<sup>5</sup>Physics Department, The University of Michigan, Ann Arbor, Michigan 48109-1040, USA

(Dated: April 16, 2024)

Coherent and dissipative interactions between different quantum systems are essential for the construction of hybrid quantum systems and the investigation of novel quantum phenomena. Here, we propose and analyze a magnon-skyrmion hybrid quantum system, consisting of a micromagnet and nearby magnetic skyrmions. We predict a strong coupling mechanism between the magnonic mode of the micromagnet and the quantized helicity degree of freedom of the skyrmion. We show that with this hybrid setup it is possible to induce magnon-mediated *nonreciprocal interactions and responses* between distant skyrmion qubits or between skyrmion qubits and other quantum systems like superconducting qubits. This work provides a quantum platform for the investigation of diverse quantum effects and quantum information processing with magnetic microstructures.

*Introduction.*—Coherent and dissipative couplings between degrees of freedom of completely different nature are the fundamental issue of quantum science and technology. These diverse types of interactions are the foundation for quantum information processing with hybrid quantum systems [1–7] and have been widely used to explore new quantum phenomena like nonreciprocal transport [8, 9] and non-Hermitian physics [10, 11]. Quantum magnonics [12–20], with the use of magnons (spin-wave quanta), provides a promising platform to study different types of quantum interactions. In particular, the magnon mode in the ferromagnetic material yttrium iron garnet (YIG) with the advantage of high spin density and low damping rate has attracted much attention [21–30]. Magnons, similar to phonons and photons [31–38], can strongly couple to various quantum systems [39–64]. Magnon-based hybrid quantum systems (such as magnon-photon [51–57], magnon-phonon [58–64], magnon-solid state spin [41–50], and magnon-superconducting qubit (SQ) hybrid setups [40, 65]), have been proposed and investigated. A plethora of interesting quantum effects have been investigated in such magnon-based quantum setups, which include the generation of non-classical states [40, 66], ground state cooling [60, 62], quantum transducers [43], multi-body entanglement [43, 59], and quantum state conversion [41, 47]. All these make quantum magnons particularly attractive for quantum technologies, and it is highly appealing to explore novel systems and novel ways of manipulating and coupling the magnetization to different degrees of freedom.

Recently, magnetic nanostructures such as skyrmions [67–72] have attracted great interests in the field of quantum science and technology [73–85]. In frustrated magnets, the skyrmion has an internal degree of freedom associated with the rotation of the helicity [86–91], and by quantizing the collective helicity coordinate, two categories of qubits can be established [92], providing a promising platform for carrying out quantum computation. However, the coupling of

this quantized helicity degree of freedom in skyrmions to other quantum systems like magnons remains largely unexplored. The investigation of coupling skyrmion qubits to other quantum degrees of freedom has its own significance and interest: First, this could enable the scalability of skyrmion qubits, since long range coherent interactions between distant skyrmions could be implemented by using the coupled quantum system as an intermediary. Second, this may allow to study novel quantum effects such as nonreciprocal quantum phenomena through the use of other useful methods like quantum reservoir engineering.

In this work, we propose and analyze a hybrid quantum system composed of a YIG micromagnet and a skyrmion, predicting that strong coupling between the magnon mode of the micromagnet and the quantized helicity degree of freedom of the skyrmion is feasible. Here, the micromagnet acts as a microwave nanomagnonic cavity to concentrate the magnonic excitations, while the skyrmion qubit behaves very similar to a superconducting charge qubit. We find that the coherent coupling between the magnonic excitation and the skyrmion qubit is well described by the Jaynes-Cummings (JC) model [93, 94]. To further enhance the coupling strength, we take into account the anisotropy of the YIG micromagnet, which results in the magnon-Kerr effect and allows the magnons to be squeezed [44, 95–97] in analogy to squeezed phonons [98–101] and photons [102–106]. Therefore, the coupling strength can be increased exponentially. By employing the magnons as an intermediary, it is possible to create tunable coherent couplings as well as dissipative couplings between distant skyrmion qubits or between skyrmion qubits and superconducting qubits. This allows for *nonreciprocal interactions and responses* between distant qubits via using the magnon-mediated dissipative coupling. For YIG micromagnets, the geometry is unspecified, which can be spherical, thin-film or even bulk. The hybrid quantum systems proposed in this work give an all-magnetic platform and greatly broaden

the avenue for quantum information processing.

*The setup.*—As illustrated in Fig. 1(a), we consider a hybrid quantum system consisting of a micromagnet and a skyrmion, where the skyrmion is located beneath the micromagnet. The micromagnet can adopt various shapes such as spheres, square or circular dots [107–111], and other configurations. Our primary focus, here, is on a hybrid system that integrates a YIG sphere with a skyrmion [the left half of Fig. 1(a)]. The vertical distances from the skyrmion to the YIG sphere’s surface and center are  $d_K$  and  $h_K$ , respectively. In the YIG sphere, long-lived spin wave modes can be excited by applying a uniform bias magnetic field  $B_K$  [112, 113]. Here, we solely take into account the Kittel mode, all spins in the micromagnet precessing in phase and with the same amplitude. The Kittel mode’s free Hamiltonian can then be expressed as  $\hat{H}_K = \omega_K \hat{s}_K^\dagger \hat{s}_K$ , where  $\hat{s}_K$  ( $\hat{s}_K^\dagger$ ) represents the annihilation (creation) operator and  $\omega_K = \gamma_e B_K$  denotes the resonance frequency (setting  $\hbar = 1$ ) [114]. The multilayer structure [138, 139], which includes square or circular dots and skyrmions as illustrated in the right half of Fig. 1(a), is discussed in detail in Ref. [114].

A skyrmion is a non-collinear spin texture with a centrosymmetric spiraling structure, as shown in Fig. S1(a). The skyrmion is located at the center of the coordinate, and its spin at position  $\tilde{\mathbf{r}} = (\tilde{x}, \tilde{y}) = (\tilde{\rho}, \phi)$  is  $\mathbf{S}$ , corresponding to the magnetic moment  $\boldsymbol{\mu}_s = -g\mu_B \mathbf{S}$  with Landé factor  $g$  and Bohr magneton  $\mu_B$ , where  $(\tilde{x}, \tilde{y})$  and  $(\tilde{\rho}, \phi)$  denote Cartesian and Polar coordinates, respectively. For a typical skyrmion, the spin direction is given by the normalized spin  $\mathbf{s} = \mathbf{S}/|\mathbf{S}| = (s_x, s_y, s_z) = [\sin \Theta(\tilde{\rho}) \cos \Phi, \sin \Theta(\tilde{\rho}) \sin \Phi, \cos \Theta(\tilde{\rho})]$ , with  $\Phi = \phi + \varphi_0$  and helicity  $\varphi_0$ . The helicity  $\varphi_0$  is the internal degree of freedom of skyrmions in frustrated magnets. The  $z$  component  $s_z$  of the normalized spin  $\mathbf{s}$  is depicted in Fig. S1(d), with the central spin oriented downward and the edge spin oriented upward. Skyrmion-based  $\mathfrak{S}_z$  qubits can be constructed by quantizing the helicity  $\varphi_0$ . Utilizing the collective coordinate quantization technique [78, 92, 114, 140–142], the Hamiltonian of  $\mathfrak{S}_z$  qubits can be represented as  $\hat{H}_{\mathfrak{S}_z} = \bar{\kappa}_z \hat{\mathfrak{S}}_z^2 - \bar{h}_z \hat{\mathfrak{S}}_z - \bar{\varepsilon}_z \cos \hat{\varphi}_0$ , with the collective coordinate  $\hat{\varphi}_0$  and its conjugate momentum  $\hat{\mathfrak{S}}_z$ , where the parameters  $\bar{\kappa}_z$ ,  $\bar{h}_z$ , and  $\bar{\varepsilon}_z$  are defined in detail in Ref. [114]. As shown in Fig. 1(b), the energy levels ( $\{|0\rangle, |1\rangle, |2\rangle, \dots\}$ ) of  $\mathfrak{S}_z$  qubits are anharmonic [92, 142], the non-harmonicity of which is generally larger than 20%. Hence, the Hamiltonian  $\hat{H}_{\mathfrak{S}_z}$  in the subspace  $\{|0\rangle, |1\rangle\}$  is given by  $\hat{H}_{\text{Sky}} = \mathcal{A}_0/2 \hat{\sigma}_z^{\text{sub}} - \mathcal{B}_0/2 \hat{\sigma}_x^{\text{sub}}$ , where  $\mathcal{A}_0 \equiv \bar{\kappa}_z - \bar{h}_z$ ,  $\mathcal{B}_0 \equiv \bar{\varepsilon}_z$ , and Pauli operators  $\hat{\sigma}_z^{\text{sub}} \equiv |1\rangle\langle 1| - |0\rangle\langle 0|$  and  $\hat{\sigma}_x^{\text{sub}} \equiv |1\rangle\langle 0| + |0\rangle\langle 1|$ .

*Interactions between the magnon and the skyrmion.*—Magnons and skyrmion qubits are coupled via magnetic fields [Fig. 1(c)]. At position  $\mathbf{r}$ , a YIG sphere with magnetic moment  $\boldsymbol{\mu} = M4\pi R_K^3/3$ , radius  $R_K$ , and magnetization  $\mathbf{M}$  produces a magnetic field that is described by  $\mathbf{B} = \frac{\mu_0}{4\pi} \left[ \frac{3\mathbf{r}(\boldsymbol{\mu} \cdot \mathbf{r})}{r^5} - \frac{\boldsymbol{\mu}}{r^3} \right]$  [143], where  $\mu_0$  is the vacuum permeability and  $\mathbf{r} = (\rho \cos \phi, \rho \sin \phi, -h_K)$  is the position vector from the magnetic sphere’s center to any point on the skyrmion

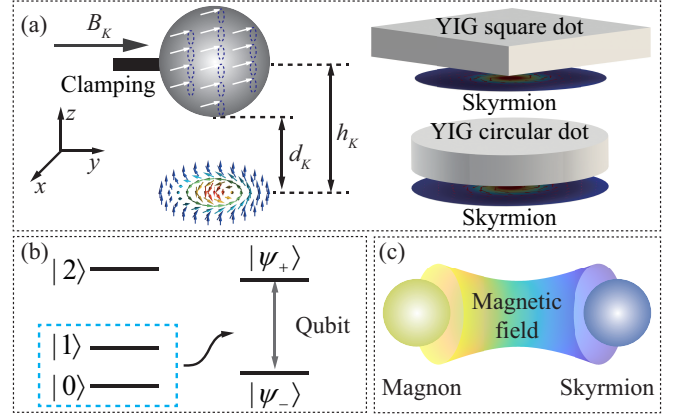


FIG. 1. (a) Hybrid quantum system consisting of a YIG sphere (a YIG square or circular dot) and a skyrmion. (b) Energy level structure of skyrmion qubits. (c) Coupling mechanisms of magnons and skyrmion qubits.

plane. By introducing the quantized magnetization operator  $\hat{\mathbf{M}} = M_K[\tilde{\mathbf{m}}_K \hat{s}_K + \tilde{\mathbf{m}}_K^* \hat{s}_K^\dagger]$ , with the Kittel mode function  $\tilde{\mathbf{m}}_K = \hat{e}_z + i\hat{e}_x$  [42, 112, 113], the quantized magnetic field generated by the YIG sphere can be expressed as  $\hat{\mathbf{B}} = (\hat{B}_x, \hat{B}_y, \hat{B}_z)$  (the detailed definition can be found in Ref. [114]). The skyrmion-magnon interaction is described by  $\hat{H}_{\text{KS}} = -g\mu_B \bar{S}/a^2 \int d\tilde{\mathbf{r}} \hat{\mathbf{B}} \cdot \mathbf{s}$  [92, 114], with  $\bar{S}$  the effective spin. By utilizing the collective operators  $\hat{\varphi}_0$  and  $\hat{\mathfrak{S}}_z$  and expanding  $\hat{H}_{\text{KS}}$  in the subspace  $\{|0\rangle, |1\rangle\}$ , the interaction Hamiltonian is reduced to

$$\hat{H}_{\text{KS}} = \frac{\lambda_{\text{KS}}^{xy}}{2} (\hat{s}_K + \hat{s}_K^\dagger) \hat{\sigma}_x^{\text{sub}} + \frac{\lambda_{\text{KS}}}{2} (\hat{s}_K + \hat{s}_K^\dagger) \hat{\sigma}_z^{\text{sub}}, \quad (1)$$

where the skyrmion-magnon coupling strength is given by [114]

$$\lambda_{\text{KS}} = \frac{2\pi g\mu_B \bar{S} \mu_0 R_K^3 M_K}{3a^3 \Lambda} \mathcal{F}(\rho) \quad (2)$$

with zero-point magnetization  $M_K = \sqrt{\hbar\gamma_e M_s/(2V_K)}$ , gyromagnetic ratio  $\gamma_e$ , saturation magnetization  $M_s$ , volume of the YIG sphere  $V_K$ , and  $\Lambda = \int d\mathbf{r} (1 - \cos \Theta_0)$ .  $\mathcal{F}(\rho)$  is a dimensionless integral [114]. The transverse coupling strength  $\lambda_{\text{KS}}^{xy}$  is presented in detail in Ref. [114].

The total Hamiltonian of the skyrmion-magnon hybrid quantum system is  $\hat{H}_{\text{TKS}} = \hat{H}_K + \hat{H}_{\text{Sky}} + \hat{H}_{\text{KS}}$ . The eigenvectors of the  $\mathfrak{S}_z$  qubit Hamiltonian  $\hat{H}_{\text{Sky}}$  are given by  $|\psi_+\rangle = \cos \theta |1\rangle - \sin \theta |0\rangle$  and  $|\psi_-\rangle = \sin \theta |1\rangle + \cos \theta |0\rangle$ , with their corresponding eigenenergies  $\mathcal{E}_\pm = \pm 1/2 \sqrt{\mathcal{A}_0^2 + \mathcal{B}_0^2}$  and  $\tan(2\theta) = \mathcal{B}_0/\mathcal{A}_0$  [Fig. 1(b)]. In the subspace  $\{|\psi_+\rangle, |\psi_-\rangle\}$ , the interaction Hamiltonian  $\hat{H}_{\text{KS}}$  can be expanded as  $\hat{H}_{\text{KS}} = \lambda_{\text{KS}}^{xy}/2 (\hat{s}_K + \hat{s}_K^\dagger) [-\sin(2\theta) \hat{\sigma}_z + \cos(2\theta) \hat{\sigma}_x] + \lambda_{\text{KS}}/2 (\hat{s}_K + \hat{s}_K^\dagger) [\cos(2\theta) \hat{\sigma}_z + \sin(2\theta) \hat{\sigma}_x]$ , with Pauli operators  $\hat{\sigma}_z = |\psi_+\rangle\langle \psi_+| - |\psi_-\rangle\langle \psi_-|$ ,  $\hat{\sigma}_+ = |\psi_+\rangle\langle \psi_-|$ , and  $\hat{\sigma}_- = |\psi_-\rangle\langle \psi_+|$ . When the  $\mathfrak{S}_z$  qubit works in the vicinity of the degeneracy point,  $\sin(2\theta) \sim 1$  and  $\cos(2\theta) \sim 0$  can be

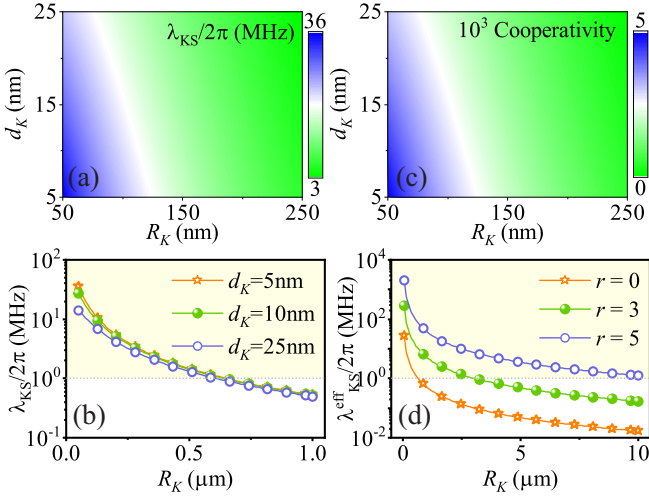


FIG. 2. Contour maps of the coupling strength  $\lambda_{KS}$  versus  $R_K$  and  $d_K$  are visualized in (a). (b) Coupling strength  $\lambda_{KS}$  as a function of  $R_K$ . (c) Contour maps of the cooperativity  $\mathcal{C}$ . The dissipation used to calculate the cooperativity is  $\gamma_K/2\pi = \gamma_{\text{sky}}/2\pi = 1$  MHz. (d) The enhanced coupling strength by the two-magnon drive ( $d_K = 10$  nm).

obtained [114]. Then, using the rotating-wave approximation the hybrid quantum system Hamiltonian becomes

$$\hat{H}_{\text{TKS}} = \frac{\omega_q}{2}\hat{\sigma}_z + \omega_K \hat{s}_K^\dagger \hat{s}_K + \bar{\lambda}_{KS} (\hat{s}_K \hat{\sigma}_+ + \hat{s}_K^\dagger \hat{\sigma}_-), \quad (3)$$

where  $\omega_q = \mathcal{E}_+ - \mathcal{E}_-$  denotes the resonant frequency of the qubit and the coupling strength is written as  $\lambda_{KS} = \lambda_{KS} \sin(2\theta)/2$ . Note that the term  $\lambda_{KS}^{xy} \sin(2\theta)/2 (\hat{s}_K + \hat{s}_K^\dagger) \hat{\sigma}_z$  has been neglected under the rotating-wave approximation, which is discussed in detail in Ref. [114].

As shown in Figs. 2(a, b), the coupling strength  $\lambda_{KS}$  is plotted as a function of the radius  $R_K$  and distance  $d_K$ . According to contour maps [Fig. 2(a)], the coupling strength can reach 20 MHz if the YIG sphere's radius can be reduced to under 100 nm. In Fig. 2(b), taking different  $d_K$ , the coupling strength  $\lambda_{KS}$  decreases with increasing  $R_K$ , and the shaded region depicts the strong-coupling regime. Here, we have assumed  $d_K = 10$  nm.  $\lambda_{KS}/2\pi$  can reach 12.7 MHz and 5.2 MHz, corresponding to  $R_K = 100$  nm and  $R_K = 200$  nm, respectively. To quantitatively analyze the system's quantum effects, we introduce the cooperativity  $\mathcal{C} = 4\lambda_{KS}^2/(\gamma_K \gamma_{\text{sky}})$  [33], where  $\gamma_K$  and  $\gamma_{\text{sky}}$  represent the dissipation of the magnon and the skyrmion, respectively. Figure 2(c) indicates that the system can reach the strong-coupling regime ( $\mathcal{C} > 1$ ) in a broad range of  $d_K$  and  $R_K$ .

*Exponentially enhanced coupling strength.*—As shown in Fig. 2(b), the radius of the YIG sphere that achieves strong coupling is  $0.6 \mu\text{m}$ . To ensure that the large-size YIG sphere still achieves strong coupling, we utilize the parametric amplification technique to enhance the coupling strength exponentially. Here, we take into account the YIG sphere's anisotropic energy, which results in the magnon-Kerr effect [95, 96]. A microwave drive is used to enhance the

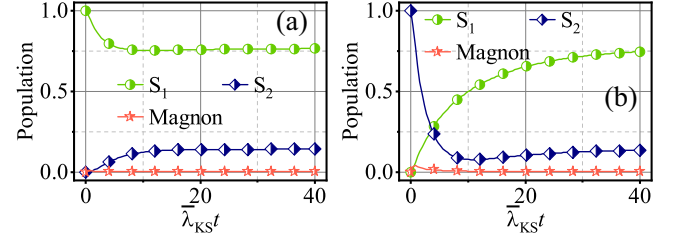


FIG. 3. Population conversion dynamics: (a) only qubit 1 in the excited state and (b) only qubit 2 in the excited state.  $S_1$  and  $S_2$  correspond to the population of the first skyrmion and second skyrmion, respectively. The parameters used are  $\Delta_{K,1} = \Delta_{q,1} = \Omega_2 = \bar{\lambda}_{KS}$  and  $\gamma_K = 10\bar{\lambda}_{KS}$ .

Kerr effect of the YIG sphere, which is described by  $\hat{H}_d = \Omega_d (\hat{s}_K^\dagger e^{-i\omega_d t} + \hat{s}_K e^{i\omega_d t})$ , with drive strength  $\Omega_d$  [44]. Under the strong microwave driving condition, the hybrid system can be described by the Hamiltonian  $\hat{H}_{\text{NKS}} = \Delta_q/2\hat{\sigma}_z + \tilde{\Delta}_K \hat{s}_K^\dagger \hat{s}_K + \bar{\lambda}_{KS} (\hat{s}_K \hat{\sigma}_+ + \hat{s}_K^\dagger \hat{\sigma}_-) - K_d/2(\hat{s}_K^{\dagger 2} + \hat{s}_K^2)$ , where  $\Delta_q = \omega_q - \omega_d$ ,  $\tilde{\Delta}_K = \Delta_K - 4K\langle \hat{s}_K \rangle^2$ , with  $\Delta_K = \omega_K - K - \omega_d$ , and the enhanced Kerr coefficient is determined by  $K_d = 2K\langle \hat{s}_K \rangle^2$ . Utilizing the Bogoliubov transformation  $\hat{m} = \hat{s}_K \cosh r - \hat{s}_K^\dagger \sinh r$ , with  $\tanh(2r) = K_d/\tilde{\Delta}_K$  [35, 98, 101, 144], the Hamiltonian  $\hat{H}_{\text{NKS}}$  can be expressed as  $\hat{H}_{\text{NKS}}^{\text{Sq}} = \Delta_q/2\hat{\sigma}_z + \Delta_K^{\text{eff}} \hat{m}^\dagger \hat{m} + \lambda_{KS}^{\text{eff}} (\hat{m} \hat{\sigma}_+ + \hat{m}^\dagger \hat{\sigma}_-)$ , where  $\Delta_K^{\text{eff}} = \tilde{\Delta}_K/\cosh(2r)$  and  $\lambda_{KS}^{\text{eff}} = \bar{\lambda}_{KS} \cosh r$ . Here we ignore the anti-rotation term  $\bar{\lambda}_{KS} \sinh r (\hat{m} \hat{\sigma}_- + \hat{m}^\dagger \hat{\sigma}_+)$  when condition  $\Delta_q, \Delta_K^{\text{eff}} \gg \bar{\lambda}_{KS} \sinh r$  is satisfied. *The coupling strength of the YIG sphere and the skyrmion qubit is enhanced exponentially with the squeezing parameter  $r$ .* The parametric amplification technique can enable strong coupling of skyrmion qubits to much larger YIG spheres with dimensions of tens of micrometers, as illustrated in Fig. 2(d).

*Nonreciprocal interactions between skyrmion qubits.*— We now consider a nonreciprocal coupling, mediated by magnons, between two skyrmion qubits. Two qubits are coupled to the same YIG sphere, one of which is driven by microwaves  $\hat{H}_{\text{qd}} = -\Omega_1 (e^{i\omega_1 t} \hat{\sigma}_-^1 + e^{-i\omega_1 t} \hat{\sigma}_+^1) - \Omega_2 (e^{i\omega_2 t} \hat{\sigma}_-^2 + e^{-i\omega_2 t} \hat{\sigma}_+^2)$ , where  $\Omega_{1/2}$  and  $\omega_{1/2}$  are the driving strength and frequency, respectively. The system's Hamiltonian, when transformed to the interaction picture of drive  $\Omega_1$ , is represented by [114]  $\hat{H}_{\text{SKSD}} = \Omega_2/2\hat{\sigma}_z^2 + \Delta_{q,1}/2\hat{\sigma}_z^2 + \Delta_{K,1} \hat{s}_K^\dagger \hat{s}_K + \bar{\lambda}_{KS}/2(\hat{s}_K + \hat{s}_K^\dagger) \hat{\sigma}_x^1 + \bar{\lambda}_{KS} (\hat{s}_K \hat{\sigma}_+^2 + \hat{s}_K^\dagger \hat{\sigma}_-^2)$  with  $\Delta_{q,1} = \omega_q - \omega_1$  and  $\Delta_{K,1} = \omega_K - \omega_1$ . In other words, the JC model and the effective Rabi model are combined in a single setup. By taking into account the large dissipation of magnons ( $\gamma_K \gg \bar{\lambda}_{KS}$ ) and eliminating the magnon mode adiabatically, the effective master equation is given by  $\dot{\hat{\rho}} = -i[\hat{H}_{\text{coh}}, \hat{\rho}] + \Gamma D[\hat{\Sigma}_-] \hat{\rho}$  including the coherent coupling of  $\hat{H}_{\text{coh}} = 1/2\mathcal{W}_1 \hat{\sigma}_z^1 + 1/2\mathcal{W}_2 \hat{\sigma}_z^2 - \mathcal{G} \hat{\sigma}_x^1 \hat{\sigma}_x^2$  and the dissipative coupling of  $\hat{\Sigma}_- = 1/2\hat{\sigma}_x^1 + \hat{\sigma}_z^2$ . The parameters  $\mathcal{W}_1$ ,  $\mathcal{W}_2$ ,  $\mathcal{G}$ , and  $\Gamma$  are defined in detail in Ref. [114]. The system's



quantum Langevin equations (QLEs) can be expressed as

$$\begin{aligned}\dot{\hat{\sigma}}_-^1 &= -\frac{\Gamma}{4}\hat{\sigma}_-^1 + \frac{\Gamma}{4}\hat{\sigma}_+^1 - \left(-\frac{\Gamma}{4}\hat{\sigma}_-^2 + \frac{\Gamma}{4}\hat{\sigma}_+^2\right)\hat{\sigma}_z^1, \\ \dot{\hat{\sigma}}_-^2 &= -\frac{\Gamma}{4}\hat{\sigma}_-^2 - \left(-\frac{\Gamma}{4}\hat{\sigma}_-^1 - \frac{\Gamma}{4}\hat{\sigma}_+^1\right)\hat{\sigma}_z^2,\end{aligned}\quad (4)$$

where we have chosen the parameters as  $\mathcal{W}_1 = \mathcal{W}_2 = \mathcal{G} = 0$ . The entire QLEs are provided in Ref. [114]. The nonlocal damping  $\Gamma$  couples the raising and lowering operators of the two qubits; in other words, the nonlocal damping induced by the engineered reservoir mediates a nonlocal damping force on each qubit. Furthermore, the dissipative coupling is asymmetric, allowing for nonreciprocal population conversion. Figures 3(a) and (b) depict the dynamics of the system's population conversion when qubits 1 and 2 are excited, respectively. When qubit 1 is excited, it is difficult for qubit 2 to receive the excitation converted by qubit 1, but conversely qubit 1 can easily get the excitation converted by qubit 2.

*Nonreciprocal interactions between skyrmion qubits and SQs.*—We consider a YIG sphere that is coupled to both a skyrmion qubit and a SQ, as described by the Hamiltonian  $\hat{H}_{\text{SKT}} = \omega_q/2\hat{\sigma}_z + \omega_{\text{Tr}}/2\hat{\sigma}_z^S + \omega_K\hat{s}_K^\dagger\hat{s}_K + \bar{\lambda}_{\text{KS}}(\hat{s}_K\hat{\sigma}_+ + \hat{s}_K^\dagger\hat{\sigma}_-) + \mathcal{J}_{\text{KT}}(\hat{s}_K\hat{\sigma}_+^S + \hat{s}_K^\dagger\hat{\sigma}_-^S)$  [114].  $\omega_{\text{Tr}}$  is the SQ's resonance frequency, and  $\mathcal{J}_{\text{KT}} = \mathcal{J}_{\text{KT}}^0 \cos(\omega_{\text{act}}t + \phi_e)$  is the coupling strength between the magnon and the SQ, which can be achieved by tuning the external fluxes [40]. In the interaction picture, the Hamiltonian  $\hat{H}_{\text{SKT}}$  is reduced to  $\hat{H}_{\text{SKT}} = \bar{\lambda}_{\text{KS}}(\hat{s}_K\hat{\mathcal{L}}_+ + \hat{s}_K^\dagger\hat{\mathcal{L}}_-)$ , where  $\hat{\mathcal{L}}_- \equiv \hat{\sigma}_- + \eta\hat{\sigma}_-^S e^{i\phi_e} = \hat{\mathcal{L}}_+^\dagger$  and  $\eta = \mathcal{J}_{\text{KT}}^0/(2\bar{\lambda}_{\text{KS}})$ . The modulation frequency and phase are represented by  $\omega_{\text{ac}}$  and  $\phi_e$ , respectively. In the large dissipation limit  $\gamma_K \gg \bar{\lambda}_{\text{KS}}, \mathcal{J}_{\text{KT}}^0$ , the magnon modes can be adiabatically eliminated, and the reduced system can be described by the master equation  $\dot{\hat{\rho}} = -i[\hat{H}_{\text{SS}}, \hat{\rho}] + \Gamma_{\text{SS}}D[\hat{\mathcal{L}}_-]\hat{\rho}$ , where  $\hat{H}_{\text{SS}} = \mathcal{G}_{\text{SS}}(\hat{\sigma}_+\hat{\sigma}_-^S + \hat{\sigma}_-\hat{\sigma}_+^S)$  is the coherent coupling between the skyrmion qubit and the SQ, which can be achieved by an auxiliary cavity. The coherent and dissipative coupling strengths are denoted by  $\mathcal{G}_{\text{SS}}$  and  $\Gamma_{\text{SS}}$ , respectively. The system's QLEs can be expressed as

$$\begin{aligned}\dot{\hat{\sigma}}_- &= -\frac{\Gamma_{\text{SS}}}{2}\hat{\sigma}_- + \left(i\mathcal{G}_{\text{SS}} + \frac{\Gamma_{\text{SS}}}{2}\eta e^{i\phi_e}\right)\hat{\sigma}_-^S\hat{\sigma}_z, \\ \dot{\hat{\sigma}}_-^S &= -\frac{\Gamma_{\text{SS}}}{2}\eta^2\hat{\sigma}_-^S + \left(i\mathcal{G}_{\text{SS}} + \frac{\Gamma_{\text{SS}}}{2}\eta e^{-i\phi_e}\right)\hat{\sigma}_-\hat{\sigma}_z^S.\end{aligned}\quad (5)$$

It is worth noting that the presence of phase  $\phi_e$  allows for a mutual balance of coherent and dissipative coupling. This can be used to achieve a nonreciprocal population conversion between two qubits. Figures 4(a) and (b) depict the nonreciprocal conversion of population between two qubits in the case of the skyrmion qubit and SQ excitation, respectively. In particular, with  $\phi_e = \pi/2$  and  $\mathcal{G}_{\text{SS}} = -\eta\Gamma_{\text{SS}}/2$ , we get  $\dot{\hat{\sigma}}_- = -\Gamma_{\text{SS}}/2\hat{\sigma}_-$  and  $\dot{\hat{\sigma}}_-^S = -\Gamma_{\text{SS}}/2\eta^2\hat{\sigma}_-^S - i\Gamma_{\text{SS}}\eta\hat{\sigma}_-\hat{\sigma}_z^S$ , indicating that the SQ is influenced by the skyrmion qubit, but conversely the skyrmion qubit is unaffected, implying that complete isolation from the SQ to the skyrmion qubit is achieved [114].

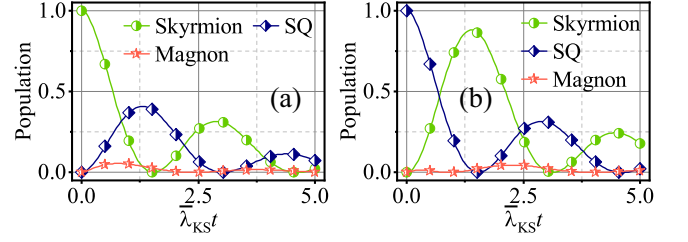


FIG. 4. Population conversion dynamics: (a) for the case of the skyrmion qubit being excited and (b) the SQ being excited. The parameters used are  $\eta = 1$ ,  $\phi_e = \pi/2$ ,  $\mathcal{G}_{\text{SS}} = \bar{\lambda}_{\text{KS}}$ , and  $\gamma_K = 10\bar{\lambda}_{\text{KS}}$ .

*Experimental feasibility.*—Utilizing the topological Hall effect, the Bloch skyrmions in frustrated magnets have been observed experimentally in triangular-lattice  $\text{Gd}_2\text{PdSi}_3$  [88] and breathing-kagomé lattice  $\text{Gd}_3\text{Ru}_4\text{Al}_{12}$  [145]. Additionally, it is expected theoretically that several candidate frustrated magnets will have skyrmions. For instance, frustrated triangular-lattice magnets with the transition-metal ions  $\text{NiGa}_2\text{S}_4$  [146, 147],  $\text{Fe}_x\text{Ni}_{1-x}\text{Br}_2$  (dihalides) [148–150], and  $\alpha\text{-NaFeO}_2$  [151, 152], where chemical substitutions can alter the anisotropy of dihalides. Furthermore,  $\text{Pb}_2\text{VO}(\text{PO}_4)_2$  [153] with a square lattice is predicted to also have skyrmions. Here the parameters of skyrmions are taken as: the effective spin  $\bar{S} = 20$ , the lattice spacing  $a = 0.5$  nm, the interaction strength  $\mathcal{J}_1 = 1$  meV, and the electric polarization  $P_E = 0.2$  C/m [92, 142]. The anisotropy energy is set to 0.13 meV, and the applied external magnetic field is given as 30 mT [92, 142]. Then we can obtain the radius of the skyrmion  $\sim 6$  nm [91]. In addition, we suppose that the applied electric field gradient is 570 V/m, which is utilized to control the skyrmion-qubit energy level spacing [90, 92]. The resonant frequency of the skyrmion qubit constructed in our model is  $\omega_q/2\pi \approx 14$  GHz.

We assume that the radius of the YIG sphere is  $R_K = 100$  nm, the saturation magnetization is  $M_s = 587$  kA/m, and the distance from the sphere's surface to the skyrmion is  $d_K = 10$  nm [41–43, 112, 113, 154]. The Kittel mode in the YIG sphere can be excited by an applied bias magnetic field  $B_K = 500$  mT [155, 156], which ensures that the YIG sphere is in saturation magnetization and is significantly larger than the magnetic field used to stabilize the skyrmion. Additionally, since homogeneous  $B_K$  contributes zero energy to skyrmions, the biased magnetic field  $B_K$  has no effect on skyrmions' stabilization [87, 92]. Then, the resonant frequency of the magnon is  $\omega_K/2\pi \approx 14$  GHz and the coupling strength of the skyrmion and the magnon is  $\lambda_{\text{KS}}/2\pi = 12.7$  MHz, which is much smaller than the non-harmonicity of the skyrmion qubit. Assuming that the dissipation of both the magnon and skyrmion qubits is 1 MHz [42, 43], the hybrid quantum system's cooperativity is  $\mathcal{C} \approx 51 \gg 1$ . Even though the dissipation of the skyrmion qubit is taken to be 10 MHz, the cooperativity  $\mathcal{C} \approx 5$  is still greater than one, i.e., the system can still reach the strong-coupling regime. For a finite

temperature  $T = 100$  mK, the equilibrium thermal magnon occupancy numbers are  $\bar{n} \approx 0.0012 \ll 1$ , and the skyrmion quits are also not thermally excited [91]. In Ref. [114], the feasibility of the proposed scheme here is further analyzed in Sec. VIII utilizing micromagnetic simulations. In addition, the calculation of the coupling strength in a multilayer structured hybrid system, composed of square or circular dots and skyrmions, is calculated in detail in Sec. IX of Ref. [114].

*Conclusion.*—We have proposed a hybrid quantum system composed of YIG micromagnets and skyrmions, and show that it can achieve the strong-coupling regime described by the JC model. We incorporate a microwave drive to make the magnons enter the nonlinear region and then employ parametric amplification techniques to achieve an exponential increase in the coupling strength. The magnon is then used as an intermediary to induce coherent and dissipative couplings between skyrmions or between skyrmions and other quantum systems. Magnon-mediated coherent couplings are utilized to improve the scalability of qubits; together with dissipative couplings, it is possible to achieve a nonreciprocal interaction and response between different qubits.

P.B.L. is supported by the National Natural Science Foundation of China under Grants No. 12375018 and No. 92065105. F.N. is supported in part by Nippon Telegraph and Telephone Corporation (NTT) Research, Japan Science, and Technology Agency (JST) (via the Quantum Leap Flagship Program (Q-LEAP), Moonshot R&D Grant No. JPMJMS2061, the Asian Office of Aerospace Research and Development (AOARD) (via Grant No. FA2386-20-1-4069), and the Foundational Questions Institute (FQXi) (via Grant No. FQXiIAF19-06). X.L.H. is Supported by the Fundamental Research Funds for the Central Universities (Program No. xzy022023002). X.Z. and M.M. acknowledge support by CREST, the Japan Science and Technology Agency (Grant No. JPMJCR20T1). M.M. also acknowledges support by the Grants-in-Aid for Scientific Research from JSPS KAKENHI (Grants No. JP20H00337 and No. 23H04522), and the Waseda University Grant for Special Research Projects (Grant No. 2023C-140).

---

\* lipengbo@mail.xjtu.edu.cn

- [1] Z.-L. Xiang, S. Ashhab, J. Q. You, and F. Nori, Hybrid quantum circuits: Superconducting circuits interacting with other quantum systems, *Rev. Mod. Phys.* **85**, 623 (2013).
- [2] M. Harder, B. M. Yao, Y. S. Gui, and C.-M. Hu, Coherent and dissipative cavity magnonics, *J. Appl. Phys.* **129**, 201101 (2021).
- [3] T. Gaebel, M. Domhan, I. Popa, C. Wittmann, P. Neumann, F. Jelezko, J. R. Rabreau, N. Stavrias, A. D. Green-tree, S. Praver, J. Meijer, J. Twamley, P. R. Hemmer, and J. Wrachtrup, Room-temperature coherent coupling of single spins in diamond, *Nat. Phys.* **2**, 408 (2006).
- [4] E. Verhagen, S. Deléglise, S. Weis, A. Schliesser, and T. J. Kippenberg, Quantum-coherent coupling of a mechanical oscillator to an optical cavity mode, *Nature (London)* **482**, 63 (2012).
- [5] F. R. Braakman, P. Barthelemy, C. Reichl, W. Wegscheider, and L. M. K. Vandersypen, Long-distance coherent coupling in a quantum dot array, *Nat. Nanotechnol.* **8**, 432 (2013).
- [6] J. J. Viennot, M. C. Dartiaillh, A. Cottet, and T. Kontos, Coherent coupling of a single spin to microwave cavity photons, *Science* **349**, 408 (2015).
- [7] T. Astner, S. Nevlacsil, N. Peterschofsky, A. Angerer, S. Rotter, S. Putz, J. Schmiedmayer, and J. Majer, Coherent coupling of remote spin ensembles via a cavity bus, *Phys. Rev. Lett.* **118**, 140502 (2017).
- [8] A. Metelmann and A. A. Clerk, Nonreciprocal photon transmission and amplification via reservoir engineering, *Phys. Rev. X* **5**, 021025 (2015).
- [9] Y.-P. Wang, J. W. Rao, Y. Yang, P.-C. Xu, Y. S. Gui, B. M. Yao, J. Q. You, and C.-M. Hu, Nonreciprocity and unidirectional invisibility in cavity magnonics, *Phys. Rev. Lett.* **123**, 127202 (2019).
- [10] W. Cao, X. Lu, X. Meng, J. Sun, H. Shen, and Y. Xiao, Reservoir-Mediated Quantum Correlations in Non-Hermitian Optical System, *Phys. Rev. Lett.* **124**, 030401 (2020).
- [11] Y. Zhang, W. Nie, and Y.-X. Liu, Edge-State Oscillations in a One-Dimensional Topological Chain with Dissipative Couplings, *Phys. Rev. Appl.* **18**, 024038 (2022).
- [12] A. V. Chumak, V. I. Vasyuchka, A. A. Serga, and B. Hillebrands, Magnon spintronics, *Nat. Phys.* **11**, 453 (2015).
- [13] Z.-X. Li, Y. Cao, and P. Yan, Topological insulators and semimetals in classical magnetic systems, *Phys. Rep.* **915**, 1 (2021).
- [14] H. Y. Yuan, Y. Cao, A. Kamra, R. A. Duine, and P. Yan, Quantum magnonics: When magnon spintronics meets quantum information science, *Phys. Rep.* **965**, 1 (2022).
- [15] B. Z. Rameshti, S. V. Kusminskiy, J. A. Haigh, K. Usami, D. Lachance-Quirion, Y. Nakamura, C.-M. Hu, H. X. Tang, G. E. Bauer, and Y. M. Blanter, Cavity magnonics, *Phys. Rep.* **979**, 1 (2022).
- [16] D. Lachance-Quirion, Y. Tabuchi, A. Gloppe, K. Usami, and Y. Nakamura, Hybrid quantum systems based on magnonics, *Appl. Phys. Express* **12**, 070101 (2019).
- [17] Y. Tabuchi, S. Ishino, A. Noguchi, T. Ishikawa, R. Yamazaki, K. Usami, and Y. Nakamura, Quantum magnonics: The magnon meets the superconducting qubit, *C. R. Phys.* **17**, 729 (2016).
- [18] M. Krawczyk and D. Grundler, Review and prospects of magnonic crystals and devices with reprogrammable band structure, *J. Phys.: Condens. Matter* **26**, 123202 (2014).
- [19] P. Pirro, V. I. Vasyuchka, A. A. Serga, and B. Hillebrands, Advances in coherent magnonics, *Nat. Rev. Mater.* **6**, 1114 (2021).
- [20] H. Yu, J. Xiao, and H. Schultheiss, Magnetic texture based magnonics, *Phys. Rep.* **905**, 1 (2021).
- [21] Y.-P. Wang, G.-Q. Zhang, D. Zhang, T.-F. Li, C.-M. Hu, and J. Q. You, Bistability of cavity magnon polaritons, *Phys. Rev. Lett.* **120**, 057202 (2018).
- [22] H. Pan, Y. Yang, Z. H. An, and C.-M. Hu, Bistability in dissipatively coupled cavity magnonics, *Phys. Rev. B* **106**, 054425 (2022).
- [23] Z.-X. Liu, H. Xiong, and Y. Wu, Magnon blockade in a hybrid ferromagnet-superconductor quantum system, *Phys. Rev. B* **100**, 134421 (2019).
- [24] H. Y. Yuan and R. A. Duine, Magnon antibunching in a nanomagnet, *Phys. Rev. B* **102**, 100402 (2020).
- [25] J.-K. Xie, S.-L. Ma, and F.-L. Li, Quantum-interference-enhanced magnon blockade in an yttrium-iron-

- garnet sphere coupled to superconducting circuits, *Phys. Rev. A* **101**, 042331 (2020).
- [26] D. Zhang, X.-Q. Luo, Y.-P. Wang, T.-F. Li, and J. Q. You, Observation of the exceptional point in cavity magnon-polaritons, *Nat. Commun.* **8**, 1368 (2017).
- [27] Y. Cao and P. Yan, Exceptional magnetic sensitivity of  $\mathcal{PT}$ -symmetric cavity magnon polaritons, *Phys. Rev. B* **99**, 214415 (2019).
- [28] G.-Q. Zhang and J. Q. You, Higher-order exceptional point in a cavity magnonics system, *Phys. Rev. B* **99**, 054404 (2019).
- [29] Z. Wang, Y. Sun, M. Wu, V. Tiberkevich, and A. Slavin, Control of spin waves in a thin film ferromagnetic insulator through interfacial spin scattering, *Phys. Rev. Lett.* **107**, 146602 (2011).
- [30] H. Qin, G.-J. Both, S. J. Hmlinen, L. Yao, and S. van Dijken, Low-loss YIG-based magnonic crystals with large tunable bandgaps, *Nat. Commun.* **9**, 5445 (2018).
- [31] M. Poot and H. S. J. van der Zant, Mechanical systems in the quantum regime, *Phys. Rep.* **511**, 273 (2012).
- [32] S. J. Whiteley, G. Wolfowicz, C. P. Anderson, A. Bourassa, H. Ma, M. Ye, G. Koolstra, K. J. Satzinger, M. V. Holt, F. J. Heremans, A. N. Cleland, D. I. Schuster, G. Galli, and D. D. Awschalom, Spin-phonon interactions in silicon carbide addressed by Gaussian acoustics, *Nat. Phys.* **15**, 490 (2019).
- [33] A. A. Clerk, K. W. Lehnert, P. Bertet, J. R. Petta, and Y. Nakamura, Hybrid quantum systems with circuit quantum electrodynamics, *Nat. Phys.* **16**, 257 (2020).
- [34] M. Perdriat, C. Pellet-Mary, P. Huillery, L. Rondin, and G. Hétet, Spin-mechanics with nitrogen-vacancy centers and trapped particles, *Micromachines* **12**, 651 (2021).
- [35] A. Blais, A. L. Grimsmo, S. M. Girvin, and A. Wallraff, Circuit quantum electrodynamics, *Rev. Mod. Phys.* **93**, 025005 (2021).
- [36] P. K. Shandilya, S. Flågan, N. C. Carvalho, E. Zohari, V. K. Kavatamane, J. E. Losby, and P. E. Barclay, Diamond integrated quantum nanophotonics: Spins, photons and phonons, *J. Lightwave Technol.* **40**, 7538 (2022).
- [37] X. Gu, A. F. Kockum, A. Miranowicz, Y.-X. Liu, and F. Nori, Microwave photonics with superconducting quantum circuits, *Phys. Rep.* **718-719**, 1 (2017).
- [38] A. F. Kockum, A. Miranowicz, S. De Liberato, S. Savasta, and F. Nori, Ultrastrong coupling between light and matter, *Nat. Rev. Phys.* **1**, 19 (2019).
- [39] Y. Tabuchi, S. Ishino, A. Noguchi, T. Ishikawa, R. Yamazaki, K. Usami, and Y. Nakamura, Coherent coupling between a ferromagnetic magnon and a superconducting qubit, *Science* **349**, 405 (2015).
- [40] M. Kounalakis, G. E. W. Bauer, and Y. M. Blanter, Analog quantum control of magnonic cat states on a chip by a superconducting qubit, *Phys. Rev. Lett.* **129**, 037205 (2022).
- [41] T. Neuman, D. S. Wang, and P. Narang, Nanomagnonic cavities for strong spin-magnon coupling and magnon-mediated spin-spin interactions, *Phys. Rev. Lett.* **125**, 247702 (2020).
- [42] X.-L. Hei, X.-L. Dong, J.-Q. Chen, C.-P. Shen, Y.-F. Qiao, and P.-B. Li, Enhancing spin-photon coupling with a micromagnet, *Phys. Rev. A* **103**, 043706 (2021).
- [43] X.-L. Hei, P.-B. Li, X.-F. Pan, and F. Nori, Enhanced tripartite interactions in spin-magnon-mechanical hybrid systems, *Phys. Rev. Lett.* **130**, 073602 (2023).
- [44] W. Xiong, M. Tian, G.-Q. Zhang, and J. Q. You, Strong long-range spin-spin coupling via a Kerr magnon interface, *Phys. Rev. B* **105**, 245310 (2022).
- [45] P. Andrich, C. F. de las Casas, X. Liu, H. L. Bretscher, J. R. Berman, F. J. Heremans, P. F. Nealey, and D. D. Awschalom, Long-range spin wave mediated control of defect qubits in nanodiamonds, *npj Quantum Inf.* **3**, 28 (2017).
- [46] D. R. Candido, G. D. Fuchs, E. Johnston-Halperin, and M. E. Flatté, Predicted strong coupling of solid-state spins via a single magnon mode, *Mater. Quantum Technol.* **1**, 011001 (2020).
- [47] M. Fukami, D. R. Candido, D. D. Awschalom, and M. E. Flatté, Opportunities for long-range magnon-mediated entanglement of spin qubits via on- and off-resonant coupling, *PRX Quantum* **2**, 040314 (2021).
- [48] I. C. Skogvoll, J. Lidal, J. Danon, and A. Kamra, Tunable anisotropic quantum rabi model via a magnon-spin-qubit ensemble, *Phys. Rev. Appl.* **16**, 064008 (2021).
- [49] C. Gonzalez-Ballester, T. van der Sar, and O. Romero-Isart, Towards a quantum interface between spin waves and paramagnetic spin baths, *Phys. Rev. B* **105**, 075410 (2022).
- [50] M. Bejarano, F. J. T. Goncalves, T. Hache, M. Hollenbach, C. Heins, T. Hula, L. Körber, J. Heinze, Y. Berencén, M. Helm, J. Fassbender, G. V. Astakhov, and H. Schultheiss, Parametric magnon transduction to spin qubits, *Sci. Adv.* **10**, eadi2042 (2024).
- [51] Ö. O. Soykal and M. E. Flatté, Strong field interactions between a nanomagnet and a photonic cavity, *Phys. Rev. Lett.* **104**, 077202 (2010).
- [52] N. J. Lambert, J. A. Haigh, and A. J. Ferguson, Identification of spin wave modes in yttrium iron garnet strongly coupled to a co-axial cavity, *J. Appl. Phys.* **117**, 053910 (2015).
- [53] D. Zhang, X.-M. Wang, T.-F. Li, X.-Q. Luo, W. Wu, F. Nori, and J. Q. You, Cavity quantum electrodynamics with ferromagnetic magnons in a small yttrium-iron-garnet sphere, *npj Quantum Inf.* **1**, 15014 (2015).
- [54] N. Kostylev, M. Goryachev, and M. E. Tobar, Superstrong coupling of a microwave cavity to yttrium iron garnet magnons, *Appl. Phys. Lett.* **108**, 062402 (2016).
- [55] S. Sharma, Y. M. Blanter, and G. E. W. Bauer, Light scattering by magnons in whispering gallery mode cavities, *Phys. Rev. B* **96**, 094412 (2017).
- [56] B. Bhoi, B. Kim, S.-H. Jang, J. Kim, J. Yang, Y.-J. Cho, and S.-K. Kim, Abnormal anticrossing effect in photon-magnon coupling, *Phys. Rev. B* **99**, 134426 (2019).
- [57] J. Xu, C. Zhong, S. Zhuang, C. Qian, Y. Jiang, A. Pishchavar, X. Han, D. Jin, J. M. Jornet, B. Zhen, J. Hu, L. Jiang, and X. Zhang, Slow-wave hybrid magnonics, *Phys. Rev. Lett.* **132**, 116701 (2024).
- [58] X. Zhang, C.-L. Zou, L. Jiang, and H. X. Tang, Cavity magnomechanics, *Sci. Adv.* **2**, e1501286 (2016).
- [59] J. Li, S.-Y. Zhu, and G. S. Agarwal, Magnon-photon-phonon entanglement in cavity magnomechanics, *Phys. Rev. Lett.* **121**, 203601 (2018).
- [60] A. Kani, B. Sarma, and J. Twamley, Intensive cavity-magnomechanical cooling of a levitated macromagnet, *Phys. Rev. Lett.* **128**, 013602 (2022).
- [61] Z. Shen, G.-T. Xu, M. Zhang, Y.-L. Zhang, Y. Wang, C.-Z. Chai, C.-L. Zou, G.-C. Guo, and C.-H. Dong, Coherent coupling between phonons, magnons, and photons, *Phys. Rev. Lett.* **129**, 243601 (2022).
- [62] M. Asjad, J. Li, S.-Y. Zhu, and J. Q. You, Magnon squeezing enhanced ground-state cooling in cavity magnomechanics, *Fundam. Res.* **3**, 3 (2023).
- [63] M. F. Colombano, G. Arregui, F. Bonell, N. E. Capuj, E. Chavez-Angel, A. Pitanti, S. O. Valenzuela, C. M. Sotomayor-Torres, D. Navarro-Urrios, and M. V. Costache, Ferromagnetic resonance assisted optomechanical magnetometer, *Phys. Rev. Lett.* **125**, 147201 (2020).



- [64] Y. Li, C. Zhao, W. Zhang, A. Hoffmann, and V. Novosad, Advances in coherent coupling between magnons and acoustic phonons, *APL Mater.* **9**, 060902 (2021).
- [65] S. P. Wolski, D. Lachance-Quirion, Y. Tabuchi, S. Kono, A. Noguchi, K. Usami, and Y. Nakamura, Dissipation-based quantum sensing of magnons with a superconducting qubit, *Phys. Rev. Lett.* **125**, 117701 (2020).
- [66] D. Xu, X.-K. Gu, H.-K. Li, Y.-C. Weng, Y.-P. Wang, J. Li, H. Wang, S.-Y. Zhu, and J. Q. You, Quantum control of a single magnon in a macroscopic spin system, *Phys. Rev. Lett.* **130**, 193603 (2023).
- [67] A. Fert, N. Reyren, and V. Cros, Magnetic skyrmions: advances in physics and potential applications, *Nat. Rev. Mater.* **2**, 17031 (2017).
- [68] K. Everschor-Sitte, J. Masell, R. M. Reeve, and M. Kläui, Perspective: Magnetic skyrmions—overview of recent progress in an active research field, *J. Appl. Phys.* **124**, 240901 (2018).
- [69] H. Ochoa and Y. Tserkovnyak, Quantum skyrmionics, *Int. J. Mod. Phys. B* **33**, 1930005 (2019).
- [70] C. Back, V. Cros, H. Ebert, K. Everschor-Sitte, A. Fert, M. Garst, T. Ma, S. Mankovsky, T. L. Monchesky, M. Mostovoy, N. Nagaosa, S. S. P. Parkin, C. Pfleiderer, N. Reyren, A. Rosch, Y. Taguchi, Y. Tokura, K. von Bergmann, and J. Zang, The 2020 skyrmionics roadmap, *J. Phys. D: Appl. Phys.* **53**, 363001 (2020).
- [71] M. Lonsky and A. Hoffmann, Dynamic excitations of chiral magnetic textures, *APL Mater.* **8**, 100903 (2020).
- [72] C. Reichhardt, C. J. O. Reichhardt, and M. V. Milošević, Statics and dynamics of skyrmions interacting with disorder and nanostructures, *Rev. Mod. Phys.* **94**, 035005 (2022).
- [73] M. Mochizuki, Spin-wave modes and their intense excitation effects in skyrmion crystals, *Phys. Rev. Lett.* **108**, 017601 (2012).
- [74] S.-Z. Lin and L. N. Bulaevskii, Quantum motion and level quantization of a skyrmion in a pinning potential in chiral magnets, *Phys. Rev. B* **88**, 060404(R) (2013).
- [75] C. Schütte and M. Garst, Magnon-skyrmion scattering in chiral magnets, *Phys. Rev. B* **90**, 094423 (2014).
- [76] A. Roldán-Molina, M. J. Santander, A. S. Nunez, and J. Fernández-Rossier, Quantum fluctuations stabilize skyrmion textures, *Phys. Rev. B* **92**, 245436 (2015).
- [77] B. Zhang, W. Wang, M. Beg, H. Fangohr, and W. Kuch, Microwave-induced dynamic switching of magnetic skyrmion cores in nanodots, *Appl. Phys. Lett.* **106**, 102401 (2015).
- [78] C. Psaroudaki, S. Hoffman, J. Klinovaja, and D. Loss, Quantum dynamics of skyrmions in chiral magnets, *Phys. Rev. X* **7**, 041045 (2017).
- [79] C. Psaroudaki and D. Loss, Skyrmions driven by intrinsic magnons, *Phys. Rev. Lett.* **120**, 237203 (2018).
- [80] A. Casiraghi, H. Corte-León, M. Vafaee, F. Garcia-Sanchez, G. Durin, M. Pasquale, G. Jakob, M. Kläui, and O. Kazakova, Individual skyrmion manipulation by local magnetic field gradients, *Commun. Phys.* **2**, 145 (2019).
- [81] D. Capic, D. A. Garanin, and E. M. Chudnovsky, Skyrmionskyrmion interaction in a magnetic film, *J. Phys.: Condens. Matter* **32**, 415803 (2020).
- [82] T. Hirose, S. A. Díaz, J. Klinovaja, and D. Loss, Magnonic quadrupole topological insulator in antiskyrmion crystals, *Phys. Rev. Lett.* **125**, 207204 (2020).
- [83] S. Khan, O. Lee, T. Dion, C. W. Zollitsch, S. Seki, Y. Tokura, J. D. Breeze, and H. Kurebayashi, Coupling microwave photons to topological spin textures in  $\text{Cu}_2\text{OSeO}_3$ , *Phys. Rev. B* **104**, L100402 (2021).
- [84] L. Liensberger, F. X. Haslbeck, A. Bauer, H. Berger, R. Gross, H. Huebl, C. Pfleiderer, and M. Weiler, Tunable cooperativity in coupled spin-cavity systems, *Phys. Rev. B* **104**, L100415 (2021).
- [85] T. Hirose, A. Mook, J. Klinovaja, and D. Loss, Magnetolectric cavity magnonics in skyrmion crystals, *PRX Quantum* **3**, 040321 (2022).
- [86] A. O. Leonov and M. Mostovoy, Multiply periodic states and isolated skyrmions in an anisotropic frustrated magnet, *Nat. Commun.* **6**, 8275 (2015).
- [87] S.-Z. Lin and S. Hayami, Ginzburg-Landau theory for skyrmions in inversion-symmetric magnets with competing interactions, *Phys. Rev. B* **93**, 064430 (2016).
- [88] T. Kurumaji, T. Nakajima, M. Hirschberger, A. Kikkawa, Y. Yamasaki, H. Sagayama, H. Nakao, Y. Taguchi, T.-h. Arima, and Y. Tokura, Skyrmion lattice with a giant topological hall effect in a frustrated triangular-lattice magnet, *Science* **365**, 914 (2019).
- [89] X. Zhang, J. Xia, Y. Zhou, X. Liu, H. Zhang, and M. Ezawa, Skyrmion dynamics in a frustrated ferromagnetic film and current-induced helicity locking-unlocking transition, *Nat. Commun.* **8**, 1717 (2017).
- [90] X. Yao, J. Chen, and S. Dong, Controlling the helicity of magnetic skyrmions by electrical field in frustrated magnets, *New J. Phys.* **22**, 083032 (2020).
- [91] J. Xia, X. Zhang, X. Liu, Y. Zhou, and M. Ezawa, Universal quantum computation based on nanoscale skyrmion helicity qubits in frustrated magnets, *Phys. Rev. Lett.* **130**, 106701 (2023).
- [92] C. Psaroudaki and C. Panagopoulos, Skyrmion qubits: A new class of quantum logic elements based on nanoscale magnetization, *Phys. Rev. Lett.* **127**, 067201 (2021).
- [93] E. T. Jaynes and F. W. Cummings, Comparison of quantum and semiclassical radiation theories with application to the beam maser, *Proc. IEEE* **51**, 89 (1963).
- [94] B. W. Shore and P. L. Knight, The Jaynes-Cummings model, *J. Mod. Opt.* **40**, 1195 (1993).
- [95] Y.-P. Wang, G.-Q. Zhang, D. Zhang, X.-Q. Luo, W. Xiong, S.-P. Wang, T.-F. Li, C.-M. Hu, and J. Q. You, Magnon Kerr effect in a strongly coupled cavity-magnon system, *Phys. Rev. B* **94**, 224410 (2016).
- [96] C. Kong, H. Xiong, and Y. Wu, Magnon-induced nonreciprocity based on the magnon Kerr effect, *Phys. Rev. Appl.* **12**, 034001 (2019).
- [97] F.-Z. Ji and J.-H. An, Kerr nonlinearity induced strong spin-magnon coupling, *Phys. Rev. B* **108**, L180409 (2023).
- [98] M.-A. Lemonde, N. Didier, and A. A. Clerk, Enhanced nonlinear interactions in quantum optomechanics via mechanical amplification, *Nat. Commun.* **7**, 11338 (2016).
- [99] W. Ge, B. C. Sawyer, J. W. Britton, K. Jacobs, J. J. Bollinger, and M. Foss-Feig, Trapped ion quantum information processing with squeezed phonons, *Phys. Rev. Lett.* **122**, 030501 (2019).
- [100] P.-B. Li, Y. Zhou, W.-B. Gao, and F. Nori, Enhancing spin-phonon and spin-spin interactions using linear resources in a hybrid quantum system, *Phys. Rev. Lett.* **125**, 153602 (2020).
- [101] S. C. Burd, R. Srinivas, H. M. Knaack, W. Ge, A. C. Wilson, D. J. Wineland, D. Leibfried, J. J. Bollinger, D. T. C. Allcock, and D. H. Slichter, Quantum amplification of boson-mediated interactions, *Nat. Phys.* **17**, 898 (2021).
- [102] X.-Y. Lü, Y. Wu, J. R. Johansson, H. Jing, J. Zhang, and F. Nori, Squeezed optomechanics with phase-matched amplification and dissipation, *Phys. Rev. Lett.* **114**, 093602 (2015).
- [103] W. Qin, A. Miranowicz, P.-B. Li, X.-Y. Lü, J. Q. You, and F. Nori, Exponentially enhanced light-matter interaction, co-

- operativities, and steady-state entanglement using parametric amplification, *Phys. Rev. Lett.* **120**, 093601 (2018).
- [104] C. Leroux, L. C. G. Govia, and A. A. Clerk, Enhancing cavity quantum electrodynamics via antisqueezing: Synthetic ultra-strong coupling, *Phys. Rev. Lett.* **120**, 093602 (2018).
- [105] P. Groszkowski, H.-K. Lau, C. Leroux, L. C. G. Govia, and A. A. Clerk, Heisenberg-limited spin squeezing via bosonic parametric driving, *Phys. Rev. Lett.* **125**, 203601 (2020).
- [106] Y.-H. Chen, W. Qin, X. Wang, A. Miranowicz, and F. Nori, Shortcuts to adiabaticity for the quantum Rabi model: Efficient generation of giant entangled cat states via parametric amplification, *Phys. Rev. Lett.* **126**, 023602 (2021).
- [107] J. Ding, C. Liu, Y. Zhang, U. Erugu, Z. Quan, R. Yu, E. McCollum, S. Mo, S. Yang, H. Ding, X. Xu, J. Tang, X. Yang, and M. Wu, Nanometer-Thick Yttrium Iron Garnet Films with Perpendicular Anisotropy and Low Damping, *Phys. Rev. Appl.* **14**, 014017 (2020).
- [108] L. Wang, Z. Lu, X. Zhao, W. Zhang, Y. Chen, Y. Tian, S. Yan, L. Bai, and M. Harder, Magnetization coupling in a YIG/GGG structure, *Phys. Rev. B* **102**, 144428 (2020).
- [109] U. Chaudhuri, N. Singh, R. Mahendiran, and A. O. Adeyeye, Tuning spin wave modes in yttrium iron garnet films with stray fields, *Nanoscale* **14**, 12022 (2022).
- [110] T. Srivastava, H. Merbouche, I. Ngouagnia Yemeli, N. Beaulieu, J. Ben Youssef, M. Muñoz, P. Che, P. Bortolotti, V. Cros, O. Klein, S. Sangiao, J. De Teresa, S. Demokritov, V. Demidov, A. Anane, C. Serpico, M. d'Aquino, and G. de Loubens, Identification of a large number of spin-wave eigenmodes excited by parametric pumping in yttrium iron garnet microdisks, *Phys. Rev. Appl.* **19**, 064078 (2023).
- [111] H. Merbouche, P. Che, T. Srivastava, N. Beaulieu, J. Ben Youssef, M. Muñoz, M. d'Aquino, C. Serpico, G. de Loubens, P. Bortolotti, A. Anane, S. O. Demokritov, and V. E. Demidov, Degenerate and non-degenerate parametric excitation in YIG nanostructures, *arXiv*. 2306.16094 (2023).
- [112] C. Gonzalez-Ballester, D. Hümmer, J. Gieseler, and O. Romero-Isart, Theory of quantum acoustomechanics and acoustomechanics with a micromagnet, *Phys. Rev. B* **101**, 125404 (2020).
- [113] C. Gonzalez-Ballester, J. Gieseler, and O. Romero-Isart, Quantum acoustomechanics with a micromagnet, *Phys. Rev. Lett.* **124**, 093602 (2020).
- [114] See Supplemental Material at <https://xxx> for more details, which includes Refs. [115-137].
- [115] A. Aharoni, *Introduction to the Theory of Ferromagnetism* (Clarendon Press, Oxford, 2000).
- [116] D. D. Stancil and A. Prabhakar, *Spin waves: Theory and applications* (Springer US, New York, 2009).
- [117] J. D. Jackson, *Classical electrodynamics* (Wiley, New York, 1975).
- [118] P. C. Fletcher and R. O. Bell, Ferrimagnetic resonance modes in spheres, *J. Appl. Phys.* **30**, 687 (1959).
- [119] P. Röschmann and H. Dötsch, Properties of magnetostatic modes in ferrimagnetic spheroids, *Phys. Status Solidi B* **82**, 11 (1977).
- [120] L. R. Walker, Magnetostatic modes in ferromagnetic resonance, *Phys. Rev.* **105**, 390 (1957).
- [121] D. Mills, Quantum theory of spin waves in finite samples, *J. Magn. Magn. Mater.* **306**, 16 (2006).
- [122] H.-B. Braun and D. Loss, Berry's phase and quantum dynamics of ferromagnetic solitons, *Phys. Rev. B* **53**, 3237 (1996).
- [123] S. Chaki and A. Bhattacharjee, Role of dissipation in the stability of a parametrically driven quantum harmonic oscillator, *J. Korean Phys. Soc.* **79**, 600 (2021).
- [124] D. Nwaigwe, On the convergence of WKB approximations of the damped Mathieu equation, *J. Math. Phys.* **62**, 062702 (2021).
- [125] T. Holstein and H. Primakoff, Field dependence of the intrinsic domain magnetization of a ferromagnet, *Phys. Rev.* **58**, 1098 (1940).
- [126] P.-B. Li, S.-Y. Gao, and F.-L. Li, Quantum-information transfer with nitrogen-vacancy centers coupled to a whispering-gallery microresonator, *Phys. Rev. A* **83**, 054306 (2011).
- [127] Y.-D. Wang and A. A. Clerk, Using interference for high fidelity quantum state transfer in optomechanics, *Phys. Rev. Lett.* **108**, 153603 (2012).
- [128] S. D. Bennett, N. Y. Yao, J. Otterbach, P. Zoller, P. Rabl, and M. D. Lukin, Phonon-induced spin-spin interactions in diamond nanostructures: Application to spin squeezing, *Phys. Rev. Lett.* **110**, 156402 (2013).
- [129] B. Li, P.-B. Li, Y. Zhou, S.-L. Ma, and F.-L. Li, Quantum microwave-optical interface with nitrogen-vacancy centers in diamond, *Phys. Rev. A* **96**, 032342 (2017).
- [130] B. Li, P.-B. Li, Y. Zhou, J. Liu, H.-R. Li, and F.-L. Li, Interfacing a topological qubit with a spin qubit in a hybrid quantum system, *Phys. Rev. Appl.* **11**, 044026 (2019).
- [131] C. D. Batista, S.-Z. Lin, S. Hayami, and Y. Kamiya, Frustration and chiral orderings in correlated electron systems, *Rep. Prog. Phys.* **79**, 084504 (2016).
- [132] H. T. Diep, Phase transition in frustrated magnetic thin film-physic at phase boundaries, *Entropy* **21**, 175 (2019).
- [133] X. Zhang, J. Xia, L. Shen, M. Ezawa, O. A. Tretiakov, G. Zhao, X. Liu, and Y. Zhou, Static and dynamic properties of bimerons in a frustrated ferromagnetic monolayer, *Phys. Rev. B* **101**, 144435 (2020).
- [134] X. Zhang, J. Xia, O. A. Tretiakov, H. T. Diep, G. Zhao, J. Yang, Y. Zhou, M. Ezawa, and X. Liu, Dynamic transformation between a skyrmion string and a bimeron string in a layered frustrated system, *Phys. Rev. B* **104**, L220406 (2021).
- [135] T. Gilbert, A phenomenological theory of damping in ferromagnetic materials, *IEEE Trans. Magn.* **40**, 3443 (2004).
- [136] M. J. Donahue and D. G. Porter, OOMMF User's Guide, Version 1.0, Interagency Report NO. NISTIR 6376 (National Institute of Standards and Technology, Gaithersburg, MD, 1999).
- [137] A. Vansteenkiste, J. Leliaert, M. Dvornik, M. Helsen, F. Garcia-Sanchez, and B. Van Waeyenberge, The design and verification of Mumax3, *AIP Adv.* **4**, 107133 (2014).
- [138] L. Sun, R. X. Cao, B. F. Miao, Z. Feng, B. You, D. Wu, W. Zhang, A. Hu, and H. F. Ding, Creating an Artificial Two-Dimensional Skyrmion Crystal by Nanopatterning, *Phys. Rev. Lett.* **110**, 167201 (2013).
- [139] D. A. Gilbert, B. B. Maranville, A. L. Balk, B. J. Kirby, P. Fischer, D. T. Pierce, J. Unguris, J. A. Borchers, and K. Liu, Realization of ground-state artificial skyrmion lattices at room temperature, *Nat. Commun.* **6**, 8462 (2015).
- [140] J. Goldstone and R. Jackiw, Quantization of nonlinear waves, *Phys. Rev. D* **11**, 1486 (1975).
- [141] N. Dorey, J. Hughes, and M. P. Mattis, Soliton quantization and internal symmetry, *Phys. Rev. D* **49**, 3598 (1994).
- [142] C. Psaroudaki and C. Panagopoulos, Skyrmion helicity: Quantization and quantum tunneling effects, *Phys. Rev. B* **106**, 104422 (2022).
- [143] J. Gieseler, A. Kabcenell, E. Rosenfeld, J. D. Schaefer, A. Safira, M. J. A. Schuetz, C. Gonzalez-Ballester, C. C. Rusconi, O. Romero-Isart, and M. D. Lukin, Single-spin magnetomechanics with levitated micromagnets, *Phys. Rev. Lett.* **124**, 163604 (2020).



- [144] S. C. Burd, R. Srinivas, J. J. Bollinger, A. C. Wilson, D. J. Wineland, D. Leibfried, D. H. Slichter, and D. T. C. Allcock, Quantum amplification of mechanical oscillator motion, *Science* **364**, 1163 (2019).
- [145] M. Hirschberger, T. Nakajima, S. Gao, L. Peng, A. Kikkawa, T. Kurumaji, M. Kriener, Y. Yamasaki, H. Sagayama, H. Nakao, K. Ohishi, K. Kakurai, Y. Taguchi, X. Yu, T.-h. Arima, and Y. Tokura, Skyrmion phase and competing magnetic orders on a breathing kagomé lattice, *Nat. Commun.* **10**, 5831 (2019).
- [146] S. Nakatsuji, Y. Nambu, H. Tonomura, O. Sakai, S. Jonas, C. Broholm, H. Tsunetsugu, Y. Qiu, and Y. Maeno, Spin disorder on a triangular lattice, *Science* **309**, 1697 (2005).
- [147] C. Stock, S. Jonas, C. Broholm, S. Nakatsuji, Y. Nambu, K. Onuma, Y. Maeno, and J.-H. Chung, Neutron-scattering measurement of incommensurate short-range order in single crystals of the  $S = 1$  triangular antiferromagnet  $\text{NiGa}_2\text{S}_4$ , *Phys. Rev. Lett.* **105**, 037402 (2010).
- [148] P. Day, A. Dinsdale, E. R. Krausz, and D. J. Robbins, Optical and neutron diffraction study of the magnetic phase diagram of  $\text{NiBr}_2$ , *J. Phys. C: Solid State Phys.* **9**, 2481 (1976).
- [149] L. Régnault, J. Rossat-Mignod, A. Adam, D. Billerey, and C. Terrier, Inelastic neutron scattering investigation of the magnetic excitations in the helimagnetic state of  $\text{NiBr}_2$ , *J. Phys. France* **43**, 1283 (1982).
- [150] M. W. Moore and P. Day, Magnetic phase diagrams and helical magnetic phases in  $M_x\text{Ni}_{1-x}\text{Br}_2$  ( $M=\text{Fe}, \text{Mn}$ ): A neutron diffraction and magneto-optical study, *J. Solid State Chem.* **59**, 23 (1985).
- [151] T. McQueen, Q. Huang, J. W. Lynn, R. F. Berger, T. Klimczuk, B. G. Ueland, P. Schiffer, and R. J. Cava, Magnetic structure and properties of the  $s = 5/2$  triangular antiferromagnet  $\alpha\text{-NaFeO}_2$ , *Phys. Rev. B* **76**, 024420 (2007).
- [152] N. Terada, D. D. Khalyavin, J. M. Perez-Mato, P. Manuel, D. Prabhakaran, A. Daoud-Aladine, P. G. Radaelli, H. S. Suzuki, and H. Kitazawa, Magnetic and ferroelectric orderings in multiferroic  $\alpha\text{-NaFeO}_2$ , *Phys. Rev. B* **89**, 184421 (2014).
- [153] A. M. Ukpong, Emergence of nontrivial spin textures in frustrated van der waals ferromagnets, *Nanomater. Nanotechnol.* **11**, 1770 (2021).
- [154] M. Fuwa, R. Sakagami, and T. Tamegai, Ferromagnetic levitation and harmonic trapping of a milligram-scale yttrium iron garnet sphere, *Phys. Rev. A* **108**, 063511 (2023).
- [155] Y. Tabuchi, S. Ishino, T. Ishikawa, R. Yamazaki, K. Usami, and Y. Nakamura, Hybridizing ferromagnetic magnons and microwave photons in the quantum limit, *Phys. Rev. Lett.* **113**, 083603 (2014).
- [156] X. Zhang, C.-L. Zou, L. Jiang, and H. X. Tang, Strongly coupled magnons and cavity microwave photons, *Phys. Rev. Lett.* **113**, 156401 (2014).